

## CHAPTER V

### RESULTS AND DISCUSSION

#### 5.1 Effect of types of cosurfactant

In order to investigate the effects of cosurfactants, n-hexanol, n-pentanol, and n-butanol were selected and individually added into the microemulsion system with concentration at  $C_{\text{Triton X-100}}/C_{\text{cosurfactant}} = 1$  while  $w_o$  were varied within the range of 7.0 to 20.0. and the reactant concentration was fixed at  $0.1 \text{ mol/dm}^3$ . All synthesis were conducted under the controlled room temperature condition.

Without cosurfactant, the microemulsion with  $w_o$  of 5.5 and reactant concentration of  $0.1 \text{ mol/dm}^3$  could provide ZnS nanoparticles with the morphology of long and short rods as well as ellipsoid shown in Figure 5.1. These ZnS nanorods have aspect ratio of approximately 80 (200-750 nm in diameter and up to  $30 \mu\text{m}$  in length). Meanwhile ellipsoidal ZnS nanoparticles have diameters in the range of about 90-200 nm. With an increase in  $w_o$  up to 11, more enhanced agglomeration of ZnS particles could be observed therefore only few nanorods would be observed. In order to identify the constituent of these synthesized products, typical EDX analysis shown in Figure 5.2 was conducted to reveal that these products are ZnS nanocrystals. The obvious X-ray fluorescence peaks at 1 and 2.3 keV exhibit the combination of Zn and S. Meanwhile, the smaller peaks at 8.6 and 9.6 keV correspond to the transition Zn  $K_{\alpha}$  and  $K_{\beta}$ , respectively.

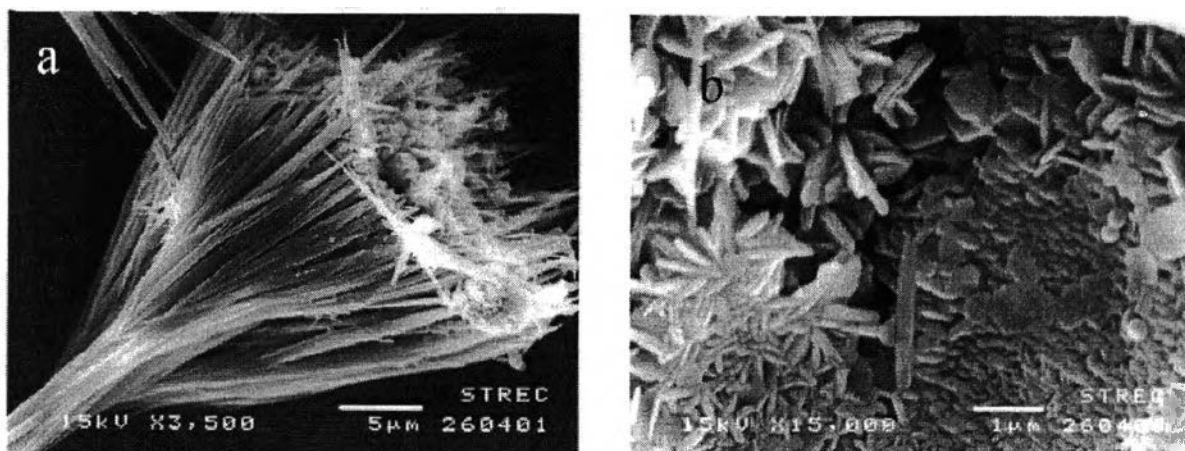


**Figure 5.1.** SEM images of ZnS nanoparticles synthesized in ternary W/O microemulsion with  $w_o=5.5$  and reactant concentration of  $0.1 \text{ mol/dm}^3$ . No cosurfactant is added.

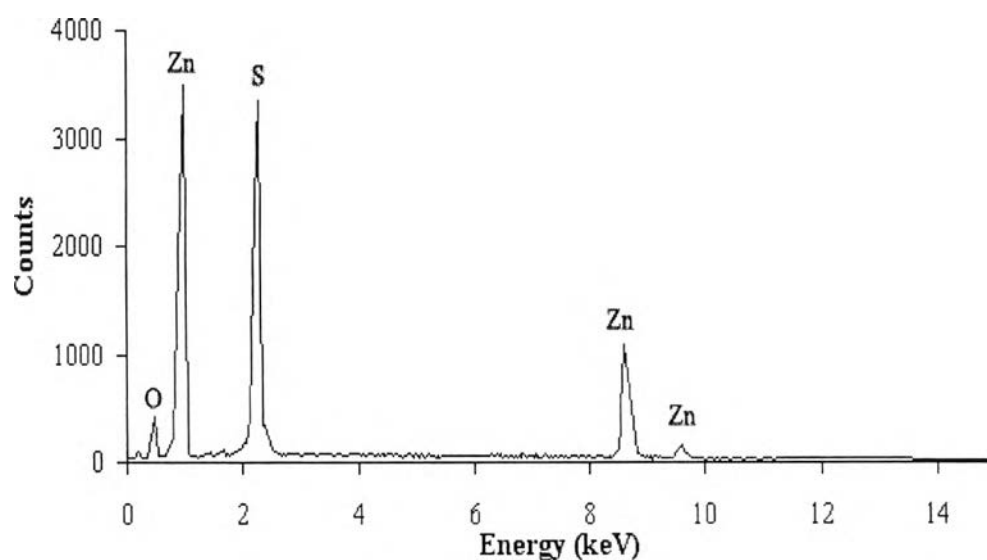


**Figure 5.2.** The EDX spectrum of typical ZnS nanoparticle samples obtained from w/o microemulsion

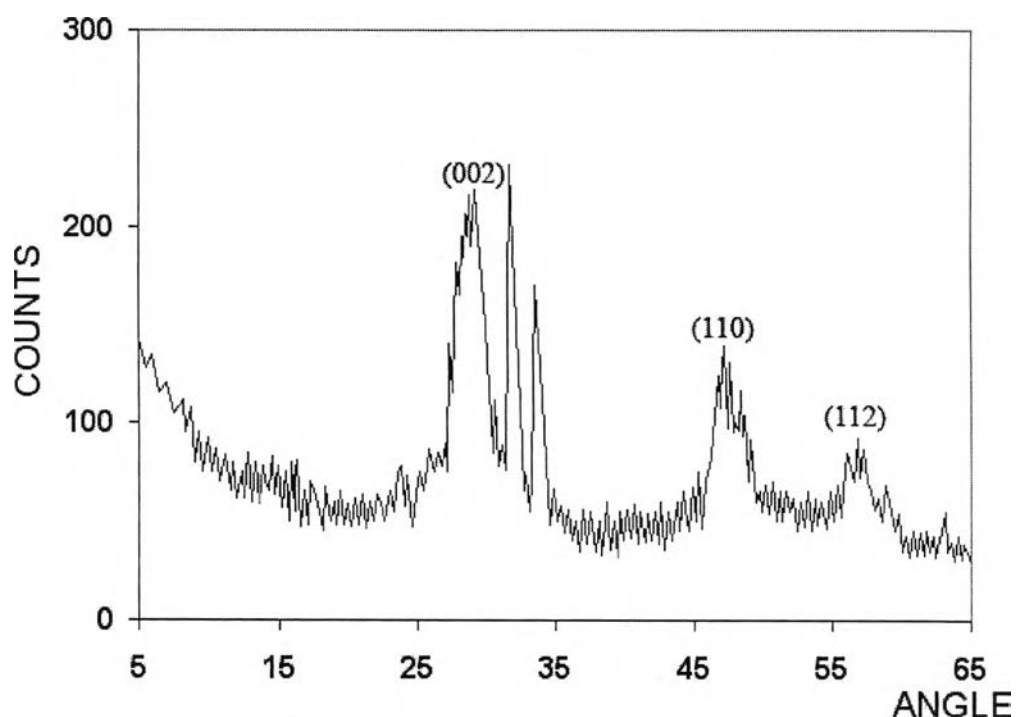


**Figure 5.3.** The XRD pattern of ZnS nanoparticles synthesized in quaternary W/O microemulsion

### 5.1.1 n-hexanol

To study the effect of cosurfactant, first the resulting products were characterized by XRD to investigate their phase. The XRD pattern show that these particles are wurtzite ZnS (Figure 5.3.). With employing n- hexanol as a cosurfactant at low  $w_o$ , Figure 5.4a and 5.4b show that the synthesized products were quantum dots with diameters smaller than 5 nm. These quantum dot particles could agglomerate to form secondary particles with larger diameters of between 40-100 nm, which however are much smaller than those obtained from heat treatment method.

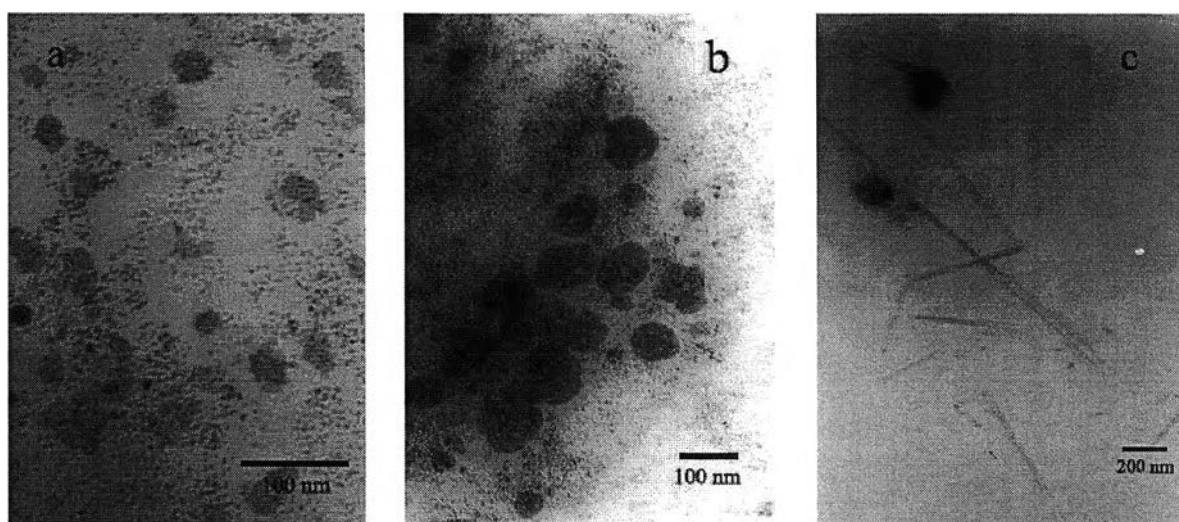


**Figure 5.4.** TEM images of ZnS nanoparticles synthesized in microemulsions with n-hexanol as a cosurfactant at : a)  $w_0=7$ , b)  $w_0=11$ , and c)  $w_0=15$

However, it is noteworthy that at  $w_0$  of 15 ZnS nanotubes with diameters of 20-40 nm and length of up to 2  $\mu\text{m}$  could be successfully synthesized (Figure 5.4c). This was very interesting morphology that hardly found when using microemulsion technique. However, this morphology were found with less quantities compared with amorphous or nanospheres.

### 5.1.2 n-pentanol

When using n-pentanol as a cosurfactant, it should be noted that there were no significant changes in the morphology of the synthesized ZnS nanoparticles at  $w_o = 7$ , comparison of Figure 5.4a and 5.5a reveals that predominant morphology of the synthesized ZnS are quantum dots and their agglomeration of which diameters are smaller than 100 nm. However, when increasing  $w_o$  value to 11 and 15 could provide ZnS nanorods and some amount of amorphous particles as shown in Figure 5.5b and 5.5c.

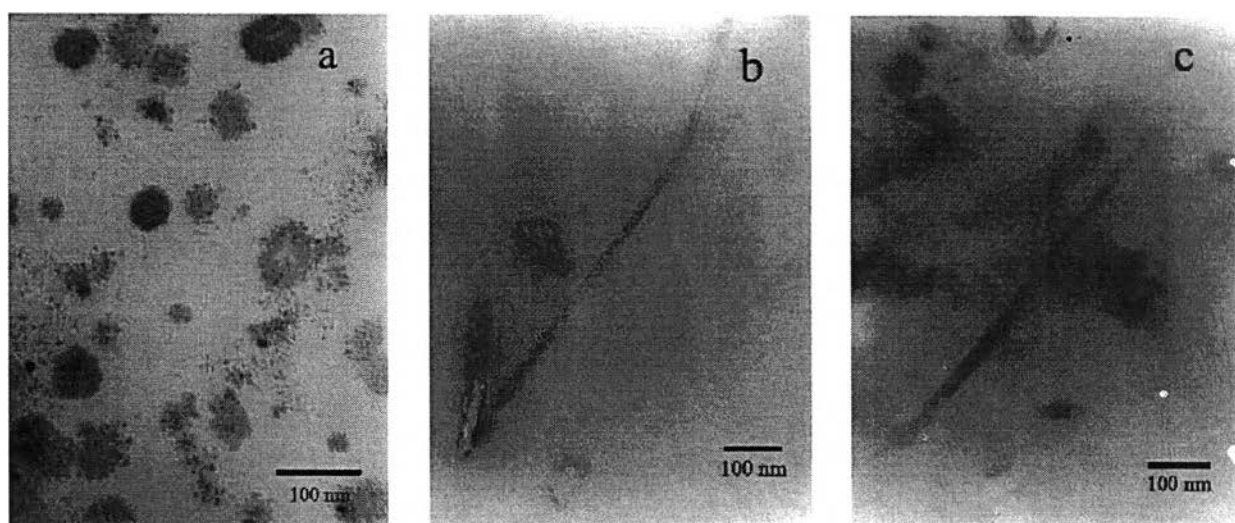


**Figure 5.5.** TEM images of ZnS nanoparticles synthesized in microemulsion with n-pentanol as a cosurfactant at: a)  $w_o=7$ , b)  $w_o=11$ , and c)  $w_o=15$ .

### 5.1.3 n-butanol

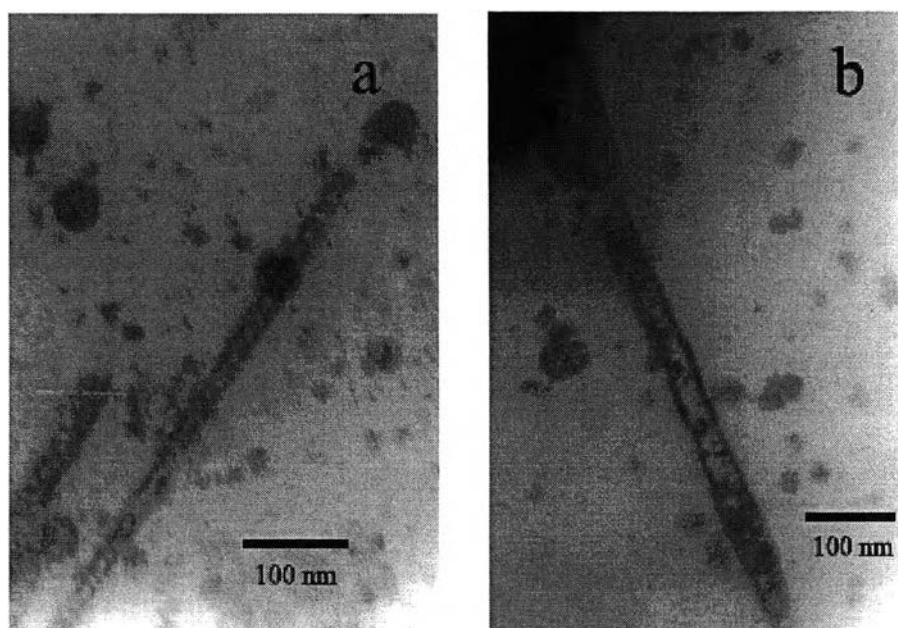


**Figure 5.6.** TEM images of ZnS nanoparticles prepared in microemulsion with n-butanol as a cosurfactant : a)  $w_0=11$ , and b)  $w_0=15$ .

When employing n-butanol as a cosurfactant, the morphology of these nanoparticles didn't change at  $w_0=7$ . However, with  $w_0$  of 11 and 15 ZnS nanotubes with some quantum dot depositing on their surface could again be successfully grown as shown in Figure 5.6a and 5.6b. And these nanotubes had larger size than when using n-hexanol as a cosurfactant but were found less than when employing n-hexanol.

## 5.2 Effect of reactant concentration

The effect of absolute reactant concentration  $[Zn^{2+}]$  and  $[S^{2-}]$  on the morphology of ZnS particles synthesized in microemulsion systems is investigated by variation in the range of 0.10 to 0.05 mol/dm<sup>3</sup>. With a decrease in the reactant concentration to 0.05 mol/dm<sup>3</sup>, the morphology of the synthesized ZnS nanoparticles will drastically change

### 5.2.1. n-hexanol

With  $w_o$  of either 11 or 20, the morphology of the ZnS nanoparticles synthesized in the microemulsion using n-hexanol as cosurfactant exhibited insignificant difference. As could be observed in Figure 5.7a and 5.7b, the agglomeration of ZnS nanoparticles, which formed larger aggregate with diameter up to 200 nm, were found spreading all over the TEM grid but no nanorods or nanotubes found.

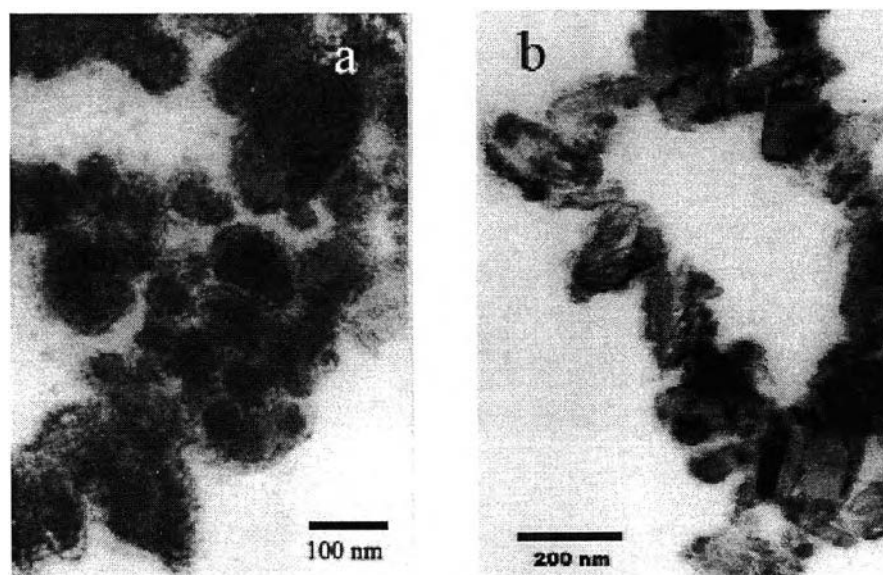


**Figure 5.7.** TEM images of ZnS nanoparticles prepared in microemulsion with n-hexanol as a cosurfactant and reactant concentration = 0.05 mol/dm<sup>3</sup>: a)  $w_o=11$ , and b)  $w_o=20$ .

### 5.2.2. n-pentanol

When employing n-pentanol as cosurfactant, at  $w_o = 11$  or 15 few ZnS nanorods with diameter of between 60 to 120 nm were found to co-exist with widely spreading ZnS quantum dots as shown in Figure 5.8a or 5.8b. From Figure 5.8c with a further increase in  $w_o$  to 20, long-nanorods no longer existed but some ellipsoidal ZnS nanoparticles and ZnS quantum dots were found to disperse thoroughly within the taken samples. The approximated diameter of these ellipsoidal nanoparticles were about 70-120 nm with the breadth of about 400 nm.

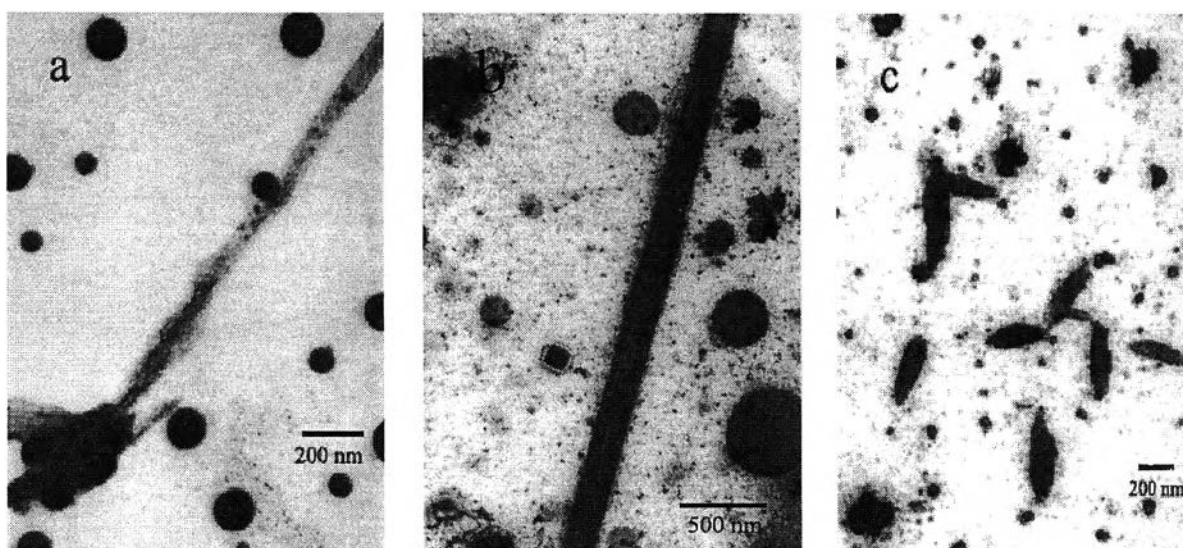


**Figure 5.8.** TEM images of ZnS nanoparticles synthesized in microemulsion with n-pentanol as a cosurfactant and reactant concentration =  $0.05 \text{ mol/dm}^3$  : a)  $w_o = 11$ , b)  $w_o = 15$ , and c), d)  $w_o = 20$



### 5.2.3 n-butanol

Finally, when n-butanol was used as a cosurfactant, the analogous trend was still observed. With lower concentration of the reactant, no ZnS nanotubes could be synthesized regardless of the increasing  $w_o$ . However, it is noteworthy that the elongated ellipsoidal morphology of ZnS nanoparticles could be obtained at  $w_o=7$  as shown in Figure 5.9a. With a further increase in  $w_o$  to 15 and 20, those ZnS nanoparticles with high aspect ratio became disappeared. Figure 5.9b and 5.9c show that only ZnS quantum dots and their agglomeration were randomly dispersed in the samples. The agglomerated nanoparticles have the approximated size of 20 – 100 nm. Also, it should be noted that further increasing  $w_o$  led to a decrease in the population density of the ZnS quantum dots but to an increase in the number of agglomeration.

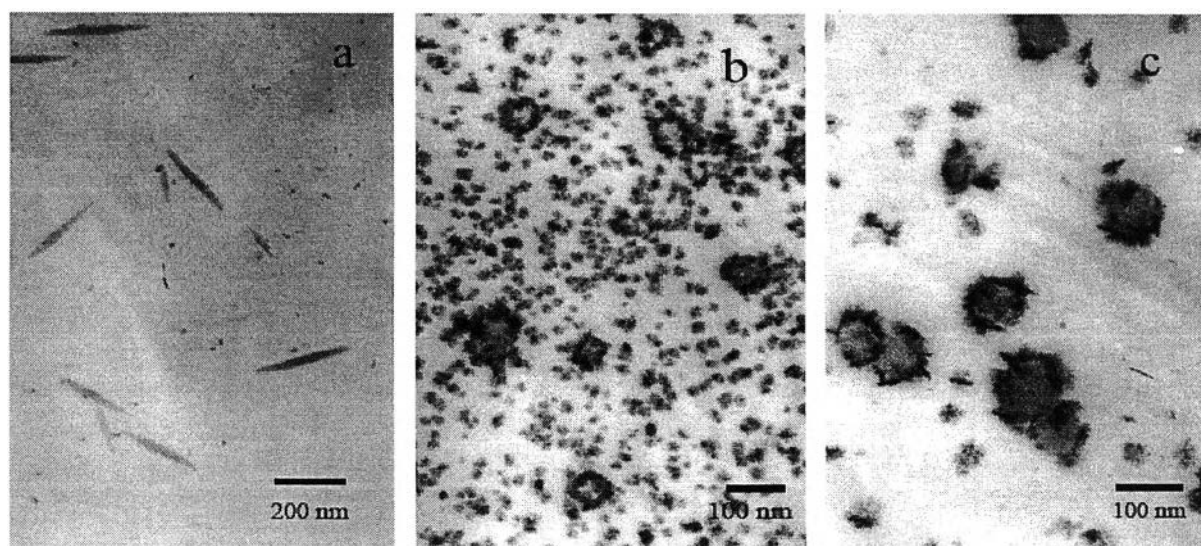
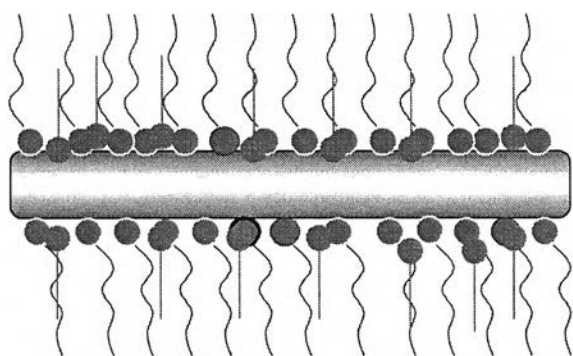
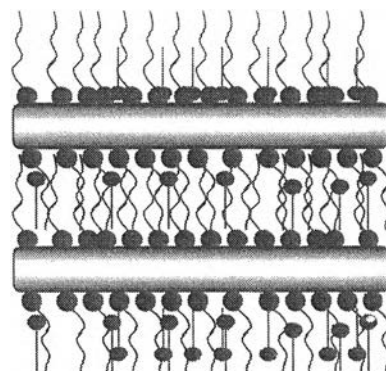


**Figure 5.9.** TEM images of ZnS nanoparticles synthesized in microemulsion with n-butanol as a cosurfactant and reactant concentration =  $0.05 \text{ mol/dm}^3$  : a)  $w_o=7$ , b)  $w_o=15$ , and c)  $w_o=20$

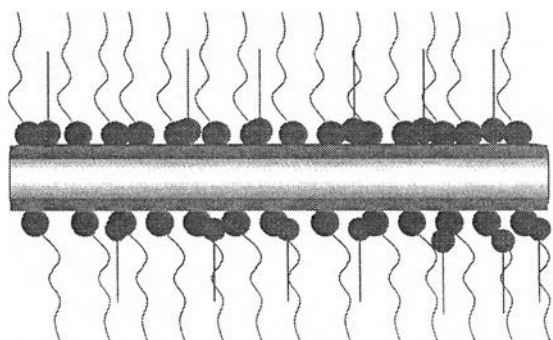
From above experimental results, it could be clearly shown that the size and the morphology of the ZnS nanoparticles are dependent upon the types of cosurfactant and the reactant concentration and the molar ratio of water to surfactant ( $w_0$ ). At high concentration of reactants and the value of  $w_0$  was more than 11, ZnS nanorods could be obtained in some cases. That can be explained by literature reviews, long rodlike micelles will be formed at high value of  $w_0$  and they act like a template. The particles will grow in these micelles to form as nanorod. For ZnS nanotubes that could be found when employing n-hexanol or n-butanol as a cosurfactant at  $w_0 = 15$ , these are very interesting morphology and hardly found when using W/O microemulsion technique to synthesize nanoparticles. The possible mechanism of this morphology can be explained as follows: Micelles with larger molecules of alcohol will have more stability and flexibility when comparing with smaller molecules of alcohol. Therefore, they have more opportunity to grow as very long rod-like micelles at a suitable condition, but their thickness of the boundary layer will be increased because of the molecule of alcohol and can hinder the reactant to diffuse into these micelles. With this implication, the reaction is occurred only at the interface between water and oil, resulting in the formation of ZnS nanotubes.



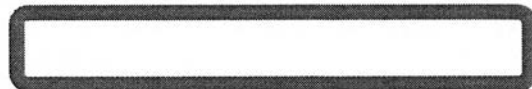
1. Rodlike micelles with cosurfactant can be formed



2. Mass transfer occurs when these micelles contact with the others



3. The reaction occurs only at the boundary layer between oil and water



4. Then nanotubes can be obtained

**Figure 5.10.** The possible mechanism of ZnS nanotubes synthesized by using w/o microemulsion technique

Moreover, when increasing the molar ratio of water to surfactant ( $w_0$ ), the number of agglomerations of ZnS nanoparticles will increase or bigger. This can simply be explained:

If we assume that these micelles are spherical, with increasing the value of  $w_0$ , the larger micelles are formed. It is possible that the layer of these micelles are weaker and able to collide with others because of their size. So, the particles in these micelles will have more opportunity to aggregate with other particles in other micelles.

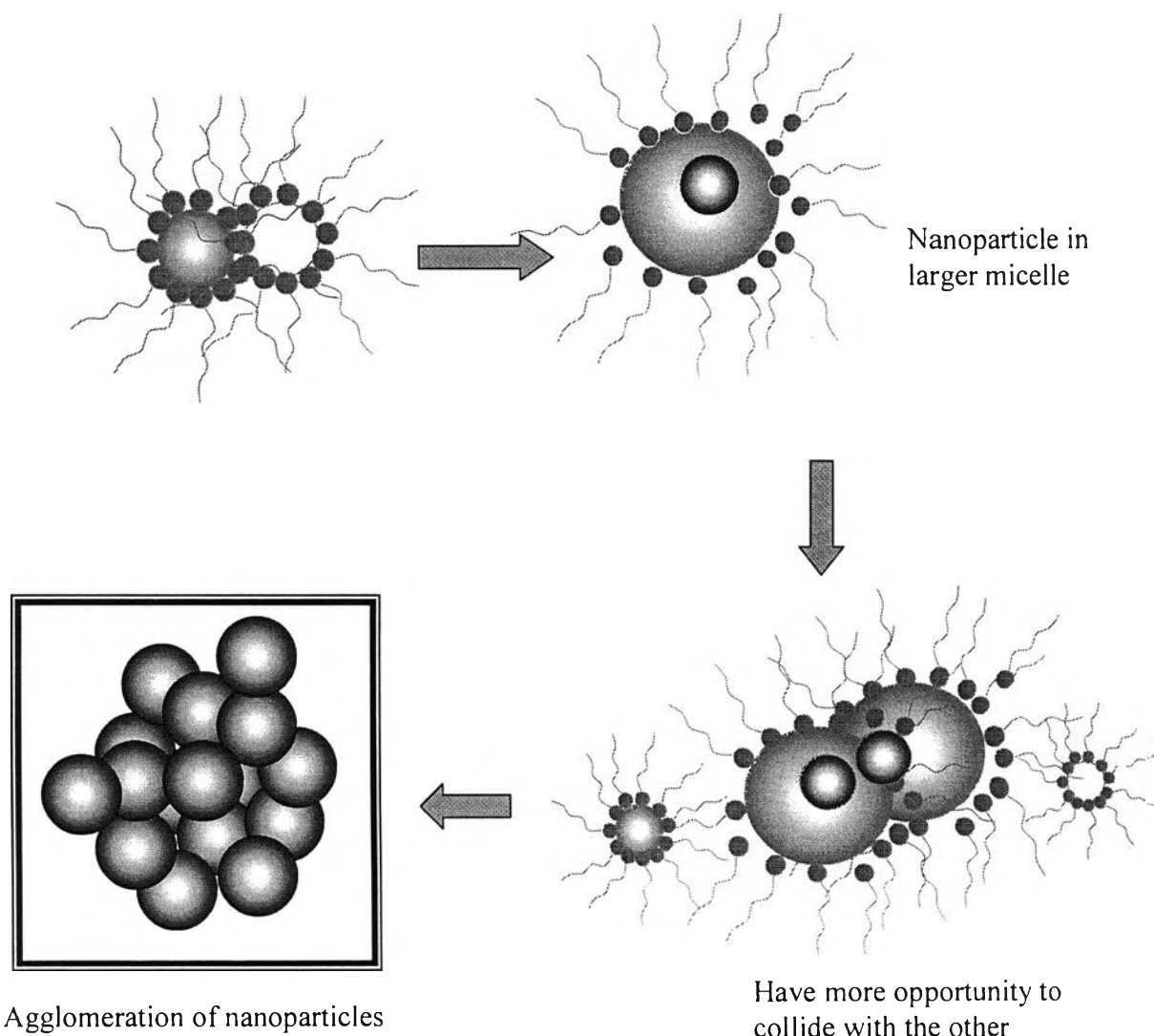


**Figure 5.11** The possible mechanism of agglomerations of ZnS nanoparticles at high  $w_0$

### 5.3. Effect of types of anions

In this study case, the reactant concentration was used only at  $0.05 \text{ mol/dm}^3$ . Before these resulting nanoparticles were investigated by TEM, XRD analysis will need to confirm that the products are ZnS. And from the result as shown in Figure 5.12 and 5.13 show that the products are wurtzite ZnS and no other inorganic compound (  $\text{ZnCl}_2$ ,  $\text{ZnBr}_2$ , NaCl or NaBr) are found.

From TEM analysis, the resulting nanoparticles when adding anions such as  $\text{Cl}^-$  or  $\text{Br}^-$  exhibited different morphology. The higher population of ZnS nanorods and nanoneedles were clearly seen from these pictures when compared in the case “ without anions ” at the same synthesis condition.

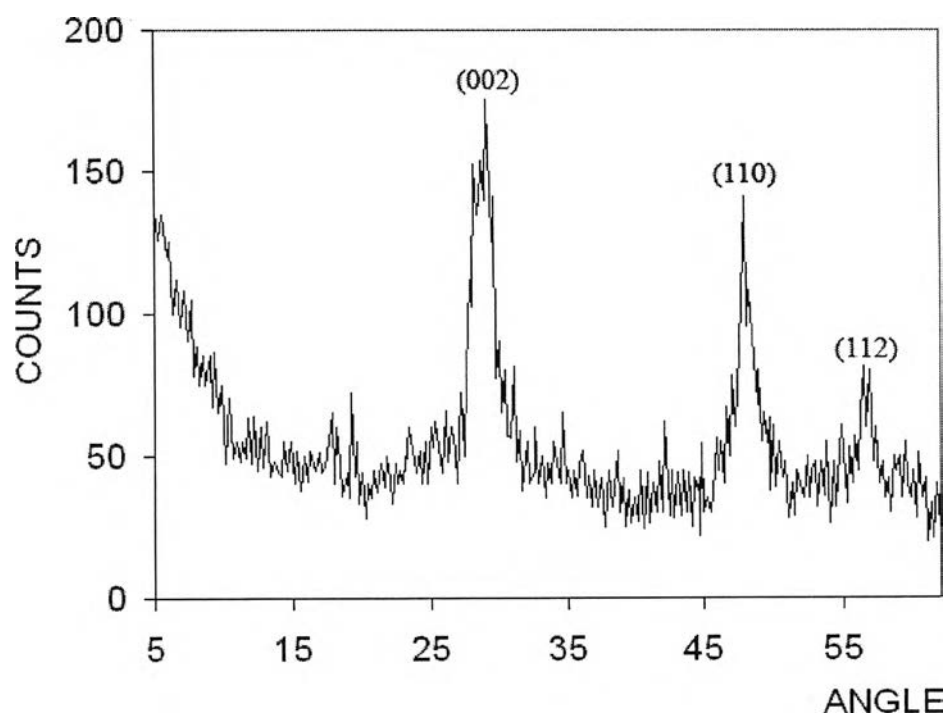


**Figure 5.12** The XRD pattern of ZnS nanoparticles synthesized in microemulsion with  $\text{Cl}^-$  as an anion

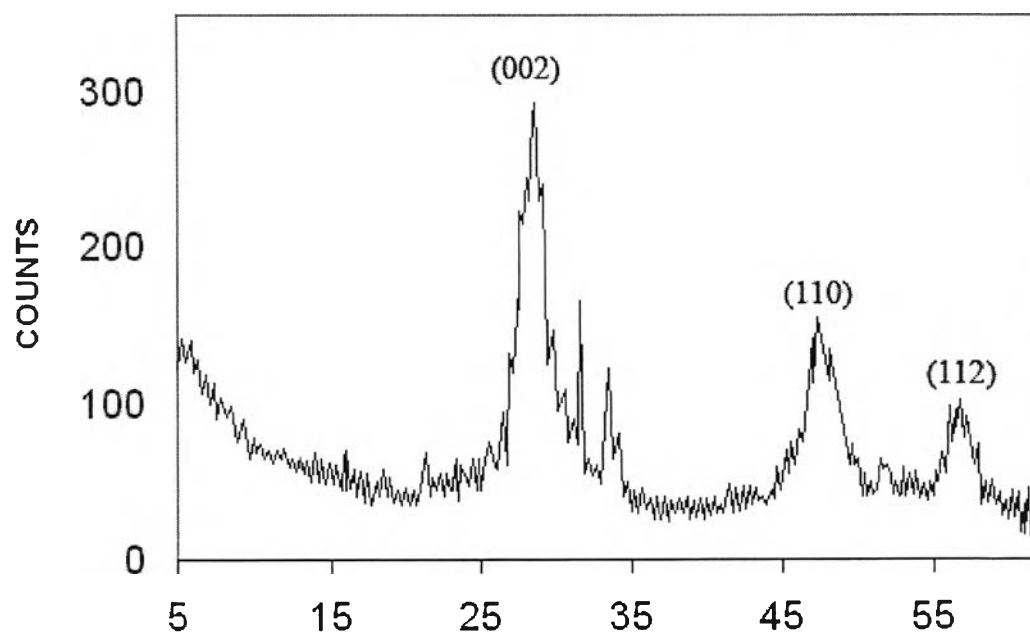


**Figure 5.13.** The XRD pattern of ZnS nanoparticles synthesized in microemulsion with  $\text{Br}^-$  as an anion

### 5.3.1 Effect of $\text{Cl}^-$

When adding  $\text{Cl}^-$  into the microemulsion with n-hexanol as a cosurfactant, ZnS nanoneedles with high aspect ratio (25-50 nm in diameter and length up to 900 nm) could be obtained at  $w_o$  of 11 (Fig. 6a). These morphologies were not found at this condition but without  $\text{Cl}^-$ . However, some amount of the agglomerations of spherical nanoparticles with the size larger than 500 nm were found too, as shown in Figure 5.14b .

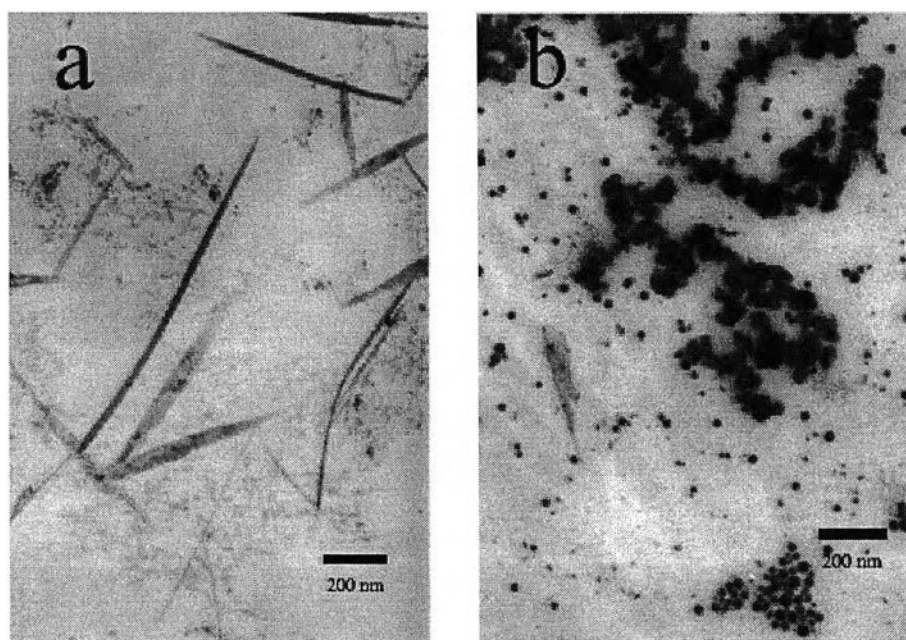


**Figure 5.14** TEM image of ZnS nanoparticles synthesized in quaternary W/O microemulsion with n-hexanol as a cosurfactant and  $\text{Cl}^-$  as an anion at  $w_o=11$ :  
a) long nanoneedles and b) nanospheres

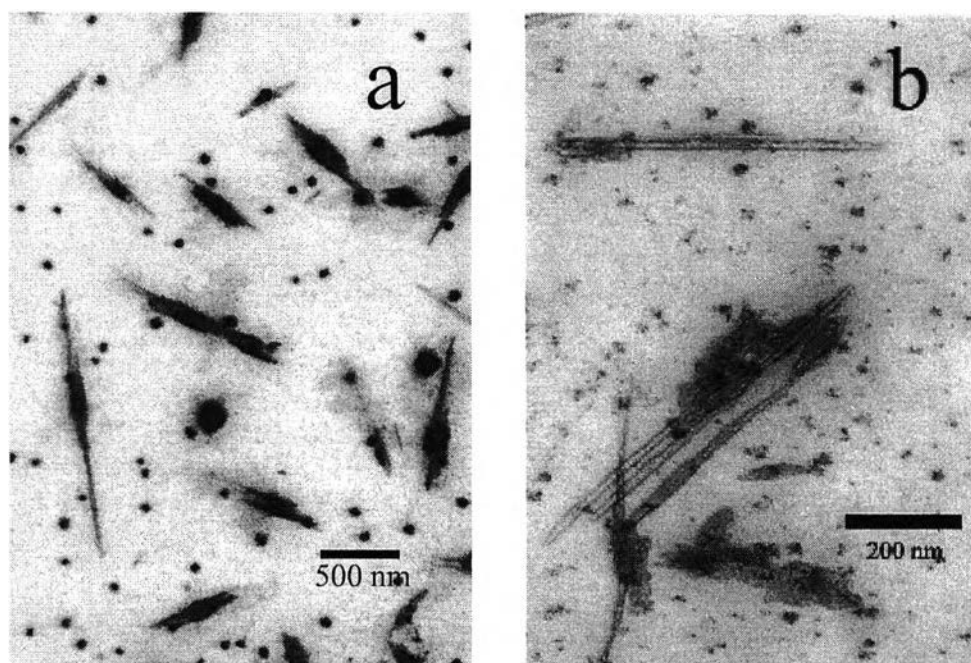


**Figure 5.15.** TEM image of ZnS nanoparticles prepared in quaternary W/O microemulsion with n-hexanol as a cosurfactant, Cl<sup>-</sup> and as anion:  $w_0=15$  a) and  $w_0=20$  b)

For increasing  $w_0$ , ZnS nanorods could be synthesized at  $w_0=15$  (Figure 5.15a). Further increasing  $w_0$  to 20, some amount of nanotubes with diameter about 15 nm were found as shown in Figure 5.15b. However, these are small amounts when comparing with the nanospheres and amorphous nanoparticles.



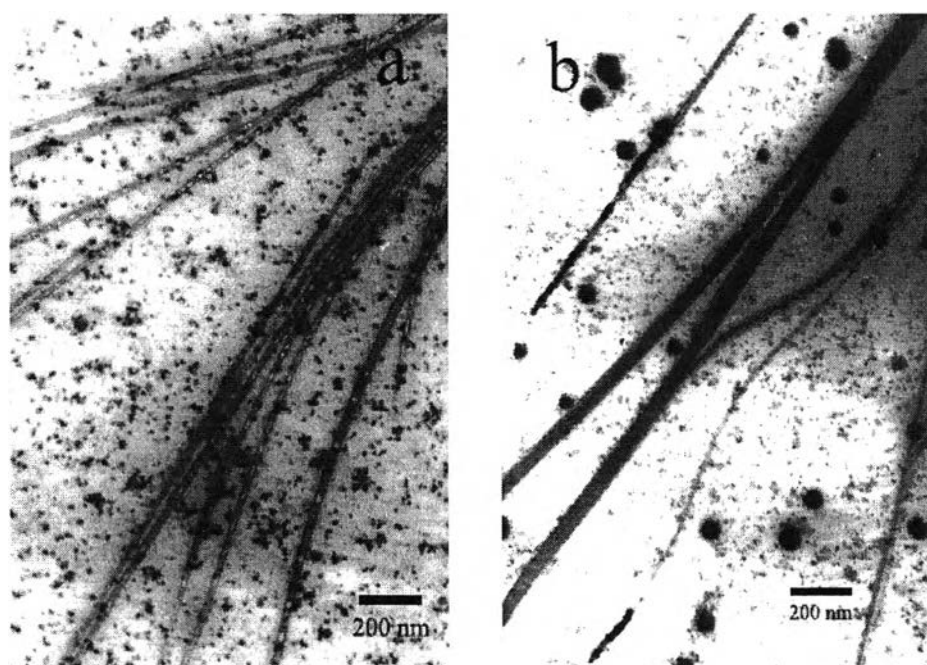


**Figure 5.16.** TEM images of ZnS nanoparticles synthesized in microemulsion with n-pentanol as a cosurfactant and  $\text{Cl}^-$  as an anion :  $w_0=11$  a), and  $w_0=15$  b).

Using n-pentanol as a cosurfactant, ZnS nanorods were obtained at  $w_0=11$ , These nanorods had an approximate diameter of 50 nm and more than 2  $\mu\text{m}$  in length. For  $w_0$  of 15, some ZnS nanorods were found too but these nanorods were not uniform in diameter. Moreover, it could be observed from these images that some amount of nanospheres coexist in this grid. However when compared with the case “without  $\text{Cl}^-$ ”, more nanorods and nanowires could be prepared and the smaller spherical nanoparticles were obtained in this case.

For employing n-butanol as a cosurfactant, the morphology of the resulting nanoparticles did not have drastically difference at  $w_o=7$  (comparing between Figure 5.9a and 5.17a). Some ZnS nanoneedles with diameter of 18 nm and length up to 120 nm (aspect ratio of 6.7) could be obtained. When increasing the value of  $w_o$  to 11, ZnS nanoneedles are slightly larger in diameter and longer as shown in Figure 5.17b.

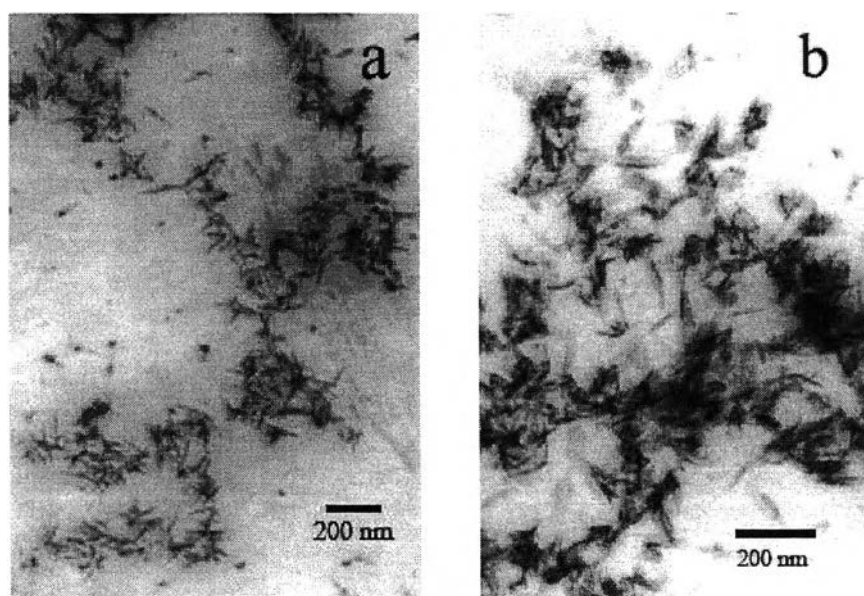


**Figure 5.17.** TEM image of ZnS nanoparticles synthesized in quaternary W/O microemulsion with n-butanol as cosurfactant and  $\text{Cl}^-$  as an anion:  $w_o=7$  a) and  $w_o=11$  b)

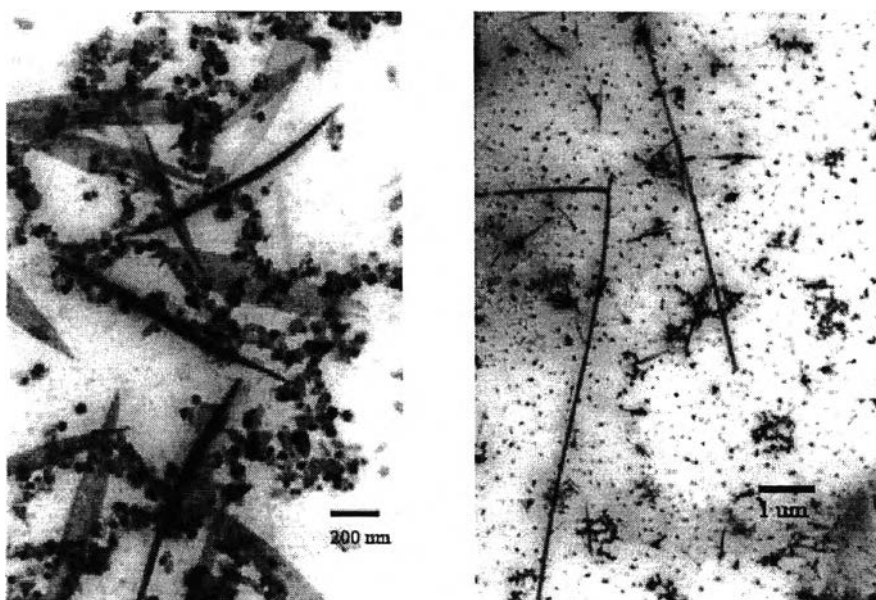


**Figure 5.18.** TEM images of ZnS nanoparticles synthesized in quaternary W/O microemulsion with n-butanol as a cosurfactant and  $\text{Cl}^-$  as an anion at  $w_0=15$

However, with further increasing the value  $w_0$  to 15, the shape of these nanoparticles significantly change when compared with the product of the case “without  $\text{Cl}^-$ ” (Figure 5.9b). ZnS nanoneedles with diameter of 64 nm and length up to 1  $\mu\text{m}$  and very long ZnS nanorods with high aspect ratio of 94 could be synthesized as shown in Figure 5.18

### 5.3.2. Effect of Br<sup>-</sup>

When adding NaBr into the microemulsion, almost nanoparticles have similar results compared with the case “with Cl<sup>-</sup>”. Some nanoparticles with higher aspect ratio are obtained.

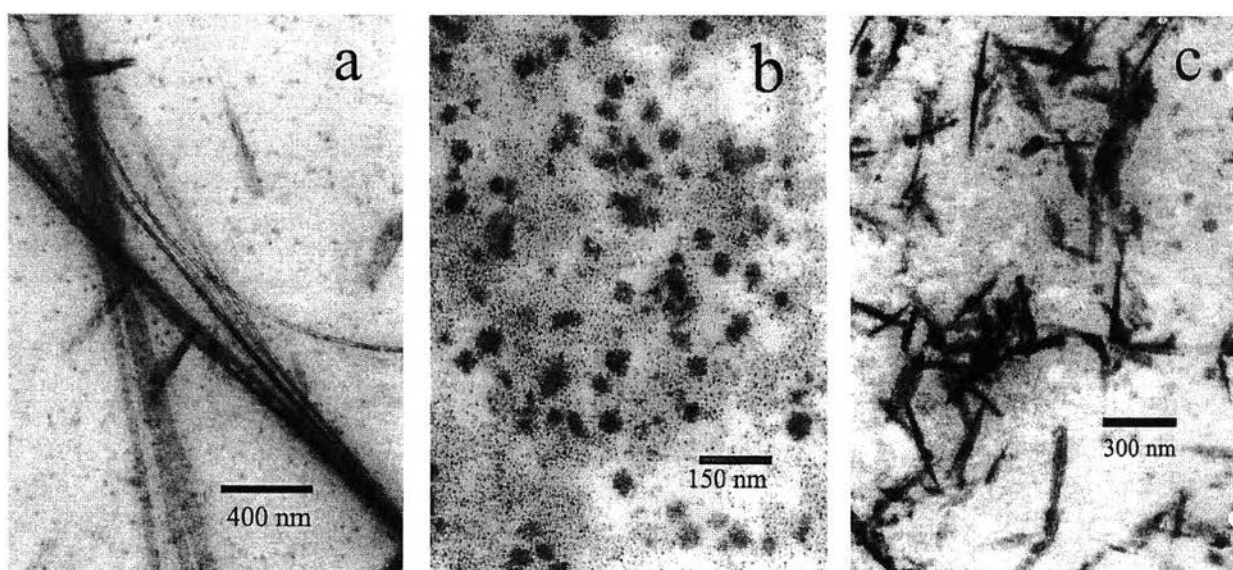


**Figure 5.19.** ZnS nanoparticles prepared in quaternary microemulsion with n-hexanol as a cosurfactant and Br<sup>-</sup> as an anion: a)  $w_o=11$ , b)  $w_o=15$ , and c)  $w_o=20$

Using n-hexanol as a cosurfactant, ZnS nanoneedles were mostly found. At  $w_o=11$ , this morphology coexist in the grid with nanowires with high aspect ratio (about 30 nm in diameter and length up to 4  $\mu\text{m}$ ). For increasing  $w_o$  to 15, the agglomerations of nanoparticles could be synthesized and no nanorods appeared. However, with a further increase in the value of  $w_o$ , some amount of nanoneedles with diameter of 30 nm were found again

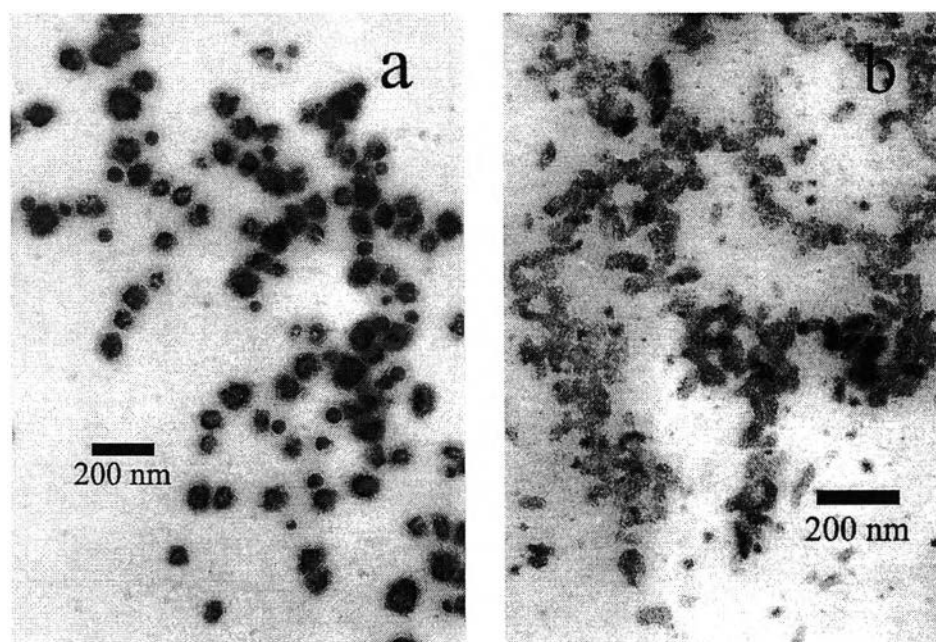


**Figure 5.20.** ZnS nanoparticles synthesized in microemulsion with n-pentanol as a cosurfactant and  $\text{Br}^-$  as an anion: a)  $w_0=11$  and b)  $w_0=15$ .

When employing n-pentanol as a cosurfactant, no ZnS nanorods were found. Some ZnS nanoparticles with diameter between 70-100 nm could be prepared at  $w_0=11$  as shown in Figure 5.20a. Meanwhile, the ellipsoidal nanoparticles could be synthesized at higher  $w_0$ . From Figure 5.20b, these nanoparticles have a size approximately of 100 nm.

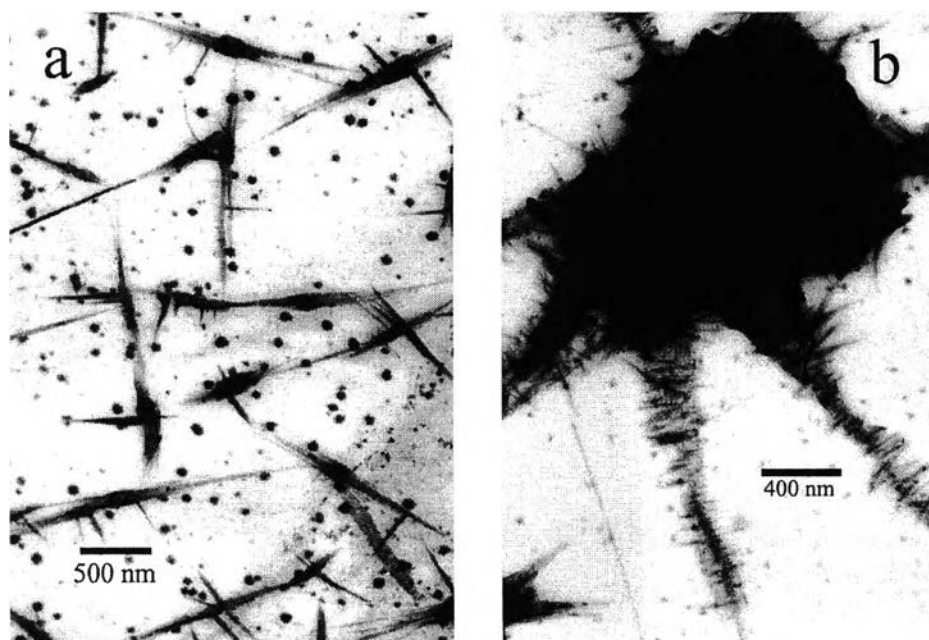


**Figure 15.21.** ZnS nanorods with some agglomeration of nanoneedles were found when using n-butanol as a cosurfactant and Br<sup>-</sup> as an anion at  $w_0=15$ .

However, ZnS nanorods with some agglomerations of nanoneedles could be synthesized when using n-butanol as a cosurfactant. This morphology of these nanoparticles is very interesting and there is no previous report available. At  $w_0 = 15$ , ZnS nanorods had diameter about 40-50 nm and up to 1.5 μm in length. The size of one nanoneedle was very small (only 30-40 in diameter and up to 400 nm in length) but the agglomerations of them could have a size larger than 2.5 μm.

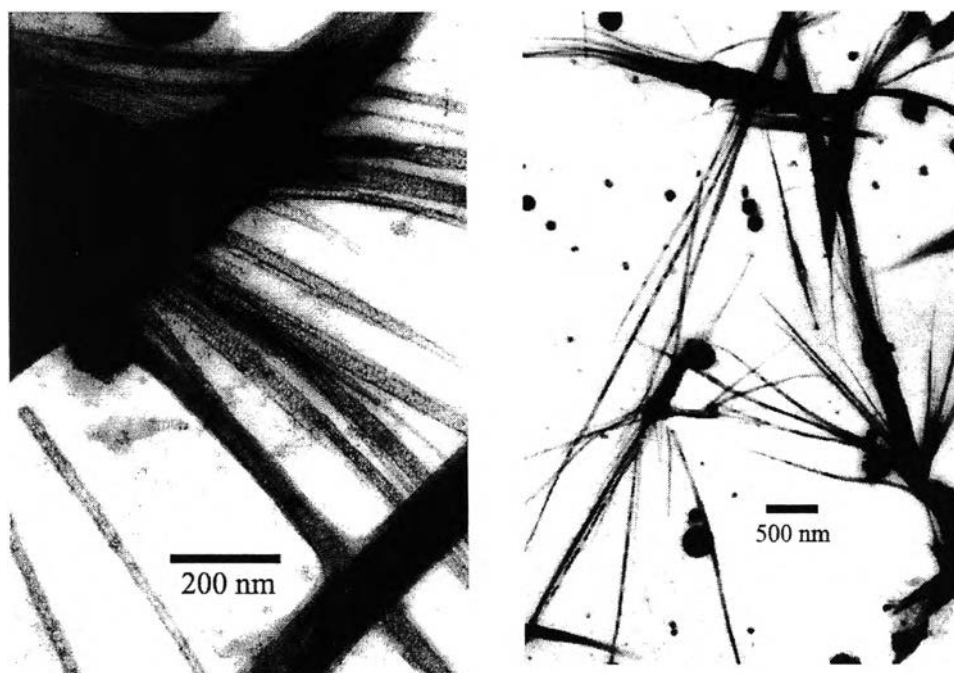


**Figure 5.22.** Agglomerations of ZnS nanowires were found when using n-butanol as a cosurfactant and  $\text{Br}^-$  as anion at  $w_0=20$ .

With higher  $w_0$ , ZnS nanoneedles were longer and grown to nanowires. As same as at  $w_0=15$ , these nanowires could aggregate as shown in Figure 5.22. These nanoparticles had diameter about 40 nm and length up to 7  $\mu\text{m}$ .

### The possible mechanism of formation in this part

From experimental results, it was clearly seen that higher population of ZnS nanoparticles with high aspect ratio were found, especially when employing n-butanol as a cosurfactant. However, it is very difficult to exactly describe the mechanism of formation in this part. From literature review, Filankembo and co-workers synthesized Cu nanocrystals and examined the effect of anions. They explained that  $\text{Cl}^-$  or  $\text{Br}^-$  could hinder Cu atom to grow in one direction, therefore more Cu nanorods were found[2]. However, in this research, we will describe the mechanism of this part in different way by using TEM analysis.

Based on the experimental results, The images of ZnS nanoparticles synthesized by microemulsion technique with n-butanol as a cosurfactant an  $\text{Br}^-$  as an anion at  $w_0=15$  or 20 were used to explain this mechanism.

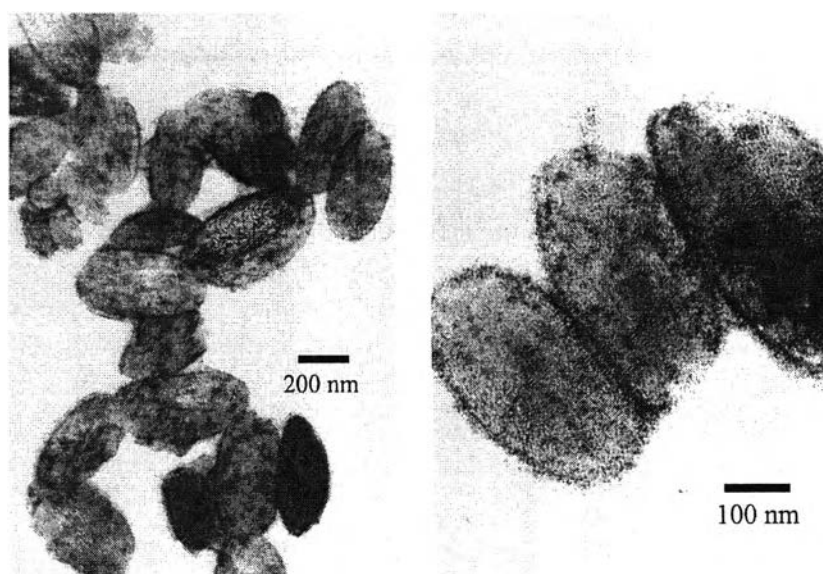


**Figure 5.23** ZnS nanoshuttles were usually found in the grid when using n-butanol as a cosurfactant and  $\text{Br}^-$  as an anion at  $w_0=15$  or 20.



First, micelles in this condition can be formed in ellipsoidal shape, this morphology of micelles can produce ZnS nanoshuttles as shown in figure 5.23. However, if  $Zn^{2+}$  atoms can not completely react with  $S^{2-}$  atom, the influence of  $Cl^-$  from the other micelles will occur when these micelles collide together. And then, when the micelle go apart from the another,  $Zn^{2+}$  atoms will be attracted and then go to the boundary layer of this micelle to react with  $S^{2-}$ . This event can change the shape of the micelle, from normal ellipsoid to longer ellipsoid. So when the reaction takes place in this micelle, ZnS nanoparticles will be controlled to form as a rod-like as shown in Figure 5.24. From these images, it could be noticed that this morphology would be formed as a nanoshuttle before growing to rod.

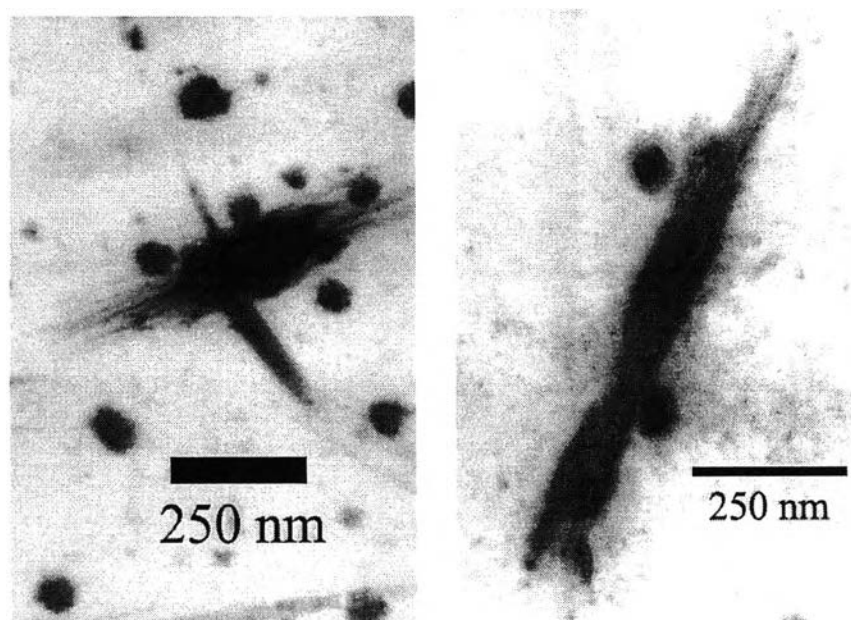
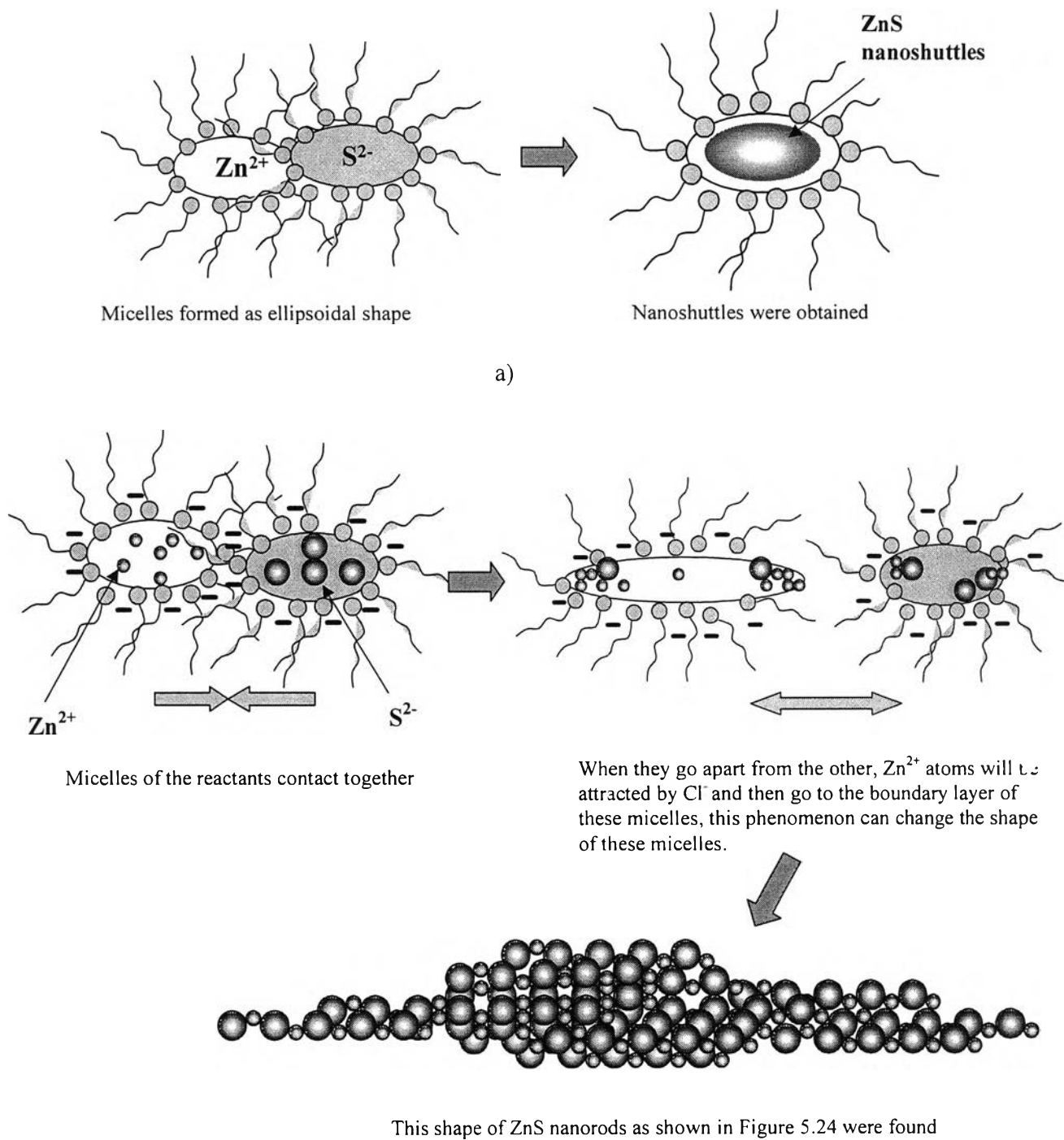


**Figure 5.24** The shape of ZnS nanorods synthesized in microemulsion with n-butanol as a cosurfactant and  $Br^-$  as an anion at  $w_o=15$  or 20.



b)

**Figure 5.25** The possible mechanism of formation of : a) ZnS nanoshuttles and b) ZnS nanorods

#### 5.4 Effect of temperature

Because temperature can affect physical properties of microemulsion, especially viscosity and phase behavior and these properties also provide great effect on mass transfer, reaction time and rate of reaction in microemulsion, therefore it could be considered as one of important parameters in synthesizing nanoparticles in microemulsion.

In this experiment, interesting results were found and these were different from preparing the experiment at room temperature. From Figure 5.23, these nanoparticles could be found when employing n-hexanol as a cosurfactant and aged at 10 °C. These distinct ZnS nanowires had very small diameter (only 5-6 nm) and up to 3 μm in length.

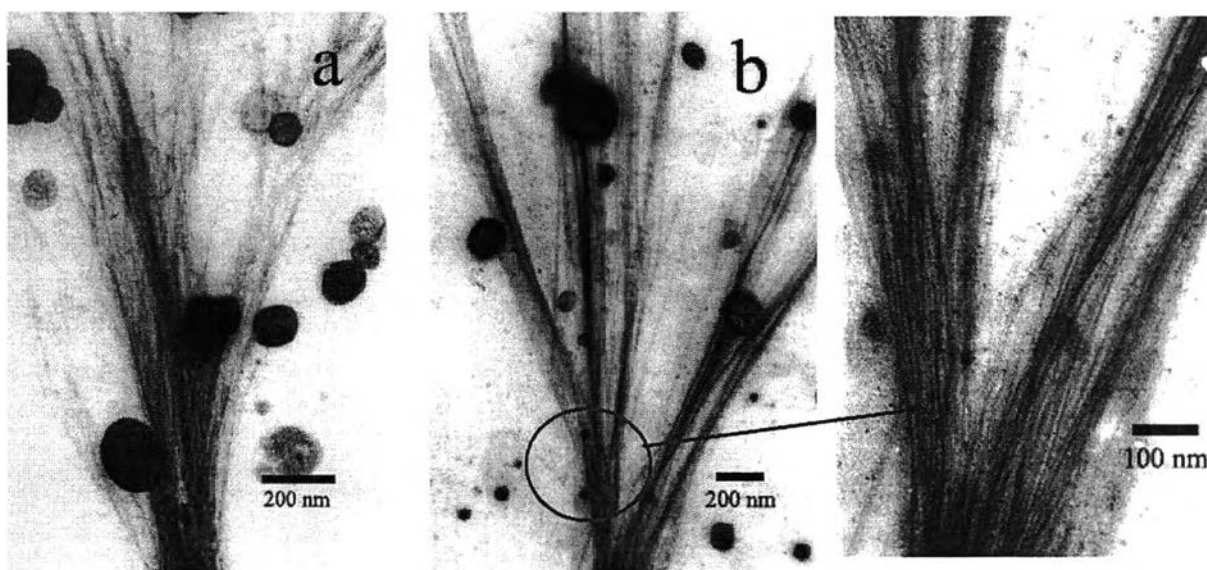


**Figure 5.26** TEM images of ZnS nanowires synthesized in microemulsion with n-hexanol as a cosurfactant and aged at temperature of 10 °C. :  $w_o=15$  a),  $w_o=20$  b) and c).

With comparison of Figure 5.23a and 5.23b, it could be found that ZnS nanowires were synthesized at  $w_0=20$  had more uniform in size and shape. However, this morphology was found with some amount of nanospheres.

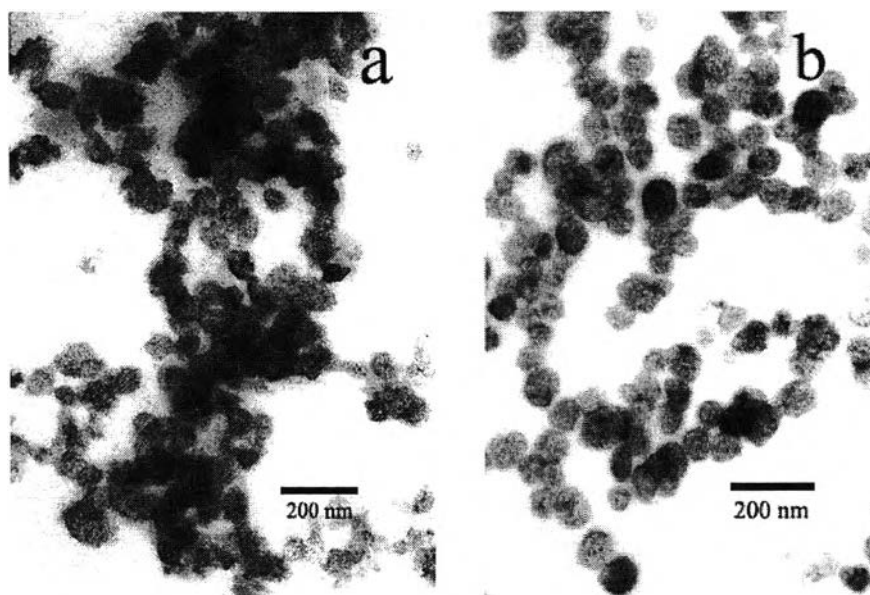


**Figure 5.27** TEM images of ZnS nanoparticles synthesized in microemulsion with n-pentanol as cosurfactant and aged at 10 °C:  $w_0=11$  a), and  $w_0=15$  b).

But when using n-pentanol as a cosurfactant and aging the obtained product at the same temperature, the morphology of nanoparticles significantly changed. As shown in Figure 5.27, the spherical nanoparticles with diameter between 40-80 nm could be obtained but ZnS nanowires were hardly found.

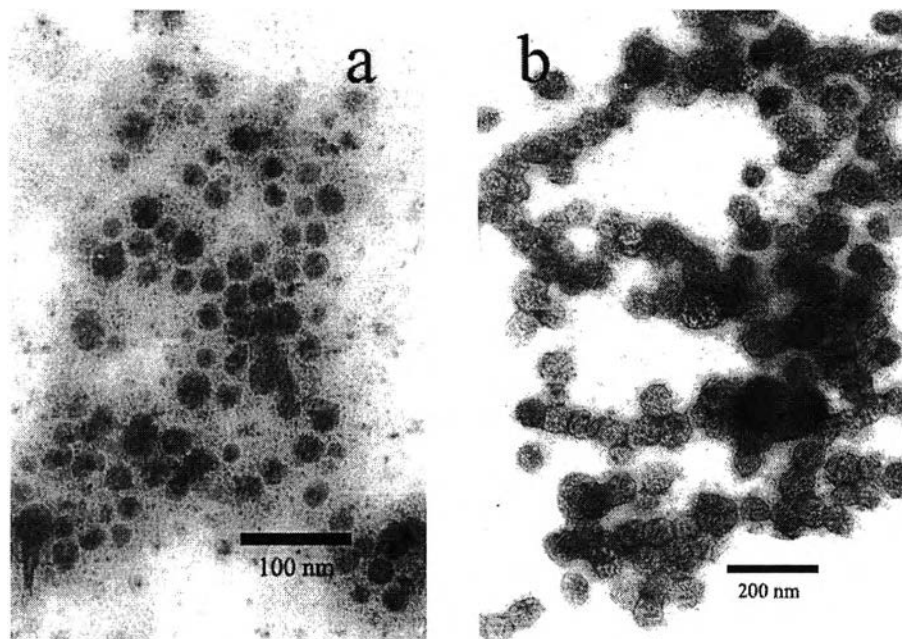


**Figure 5.28** TEM images of ZnS nanoparticles synthesized in microemulsion with n-hexanol as cosurfactant and the reaction occurred at 60 °C:  $w_o=11$  a), and  $w_o=15$  b).

For using the reaction temperature of 60 °C with n-hexanol as a cosurfactant, ZnS nanoparticles with uniform size about 20-40 nm were found at  $w_o=11$ , for increasing the value of  $w_o$  to 15, the larger nanoparticles with a diameter between 50-80 nm were obtained. In this condition, no ZnS nanowires were found.

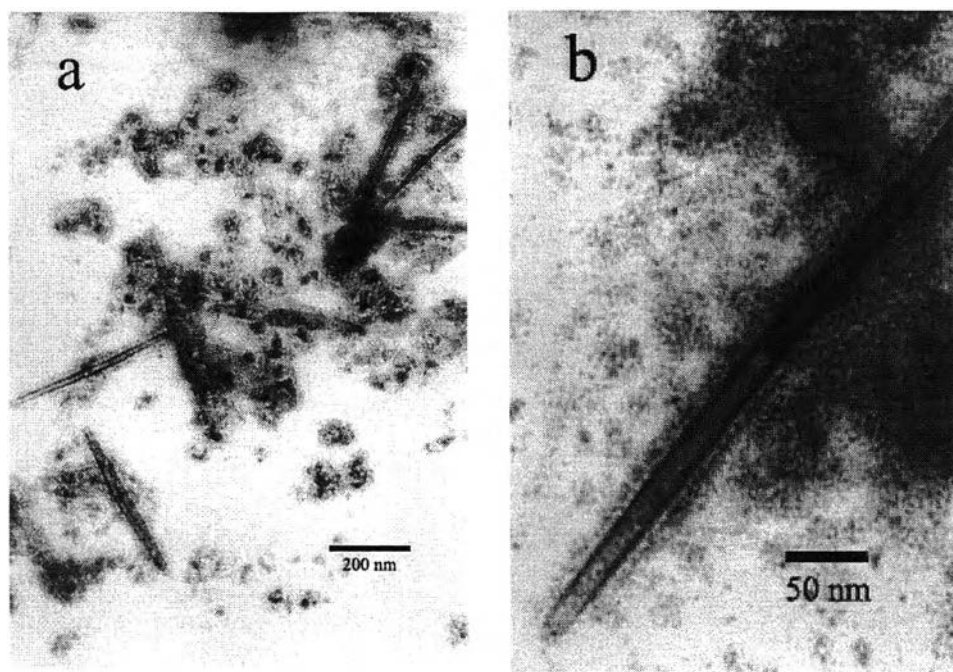


**Figure 5.29** TEM images of ZnS nanotubes synthesized in microemulsion with n-butanol as cosurfactant,  $w_o=11$  and the reaction occurred at  $60\text{ }^\circ\text{C}$

However, when using n-butanol as a cosurfactant, unexpected ZnS nanotubes were found on this grid with some amount of amorphous nanoparticles as shown in Figure 5.26a. This morphology had diameter of 20 nm and up to 450 nm in length (Figure 5.26b). For increasing  $w_o$  to 15, some nanowires with very small diameter were found again.

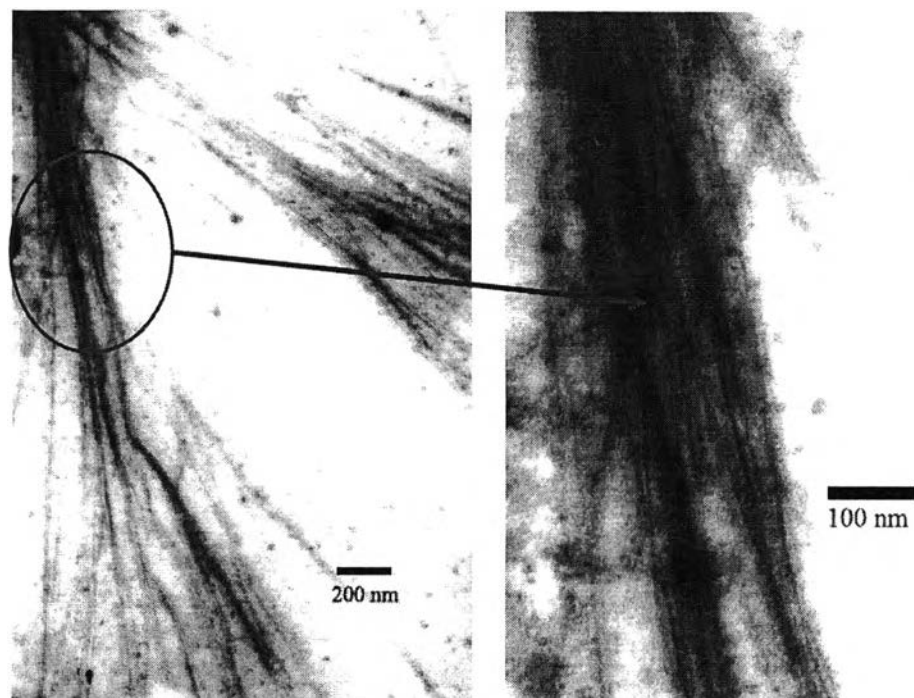


**Figure 5.30** TEM images of ZnS nanowires synthesized in microemulsion with n-butanol as cosurfactant,  $w_o=15$  and the reaction temperature = 60 °C.

### 5.5 Particle size distribution by DLS

As mentioned above, the size distribution of each ZnS in microemulsion was measured by DLS technique. In this work, this analysis was used for examining the size of particles in microemulsion and confirm as TEM images. Based on experimental results, the hydrodynamic diameters of the resulting nanoparticles are in a range of 80-1500 nm which are higher than TEM analysis due to the agglomeration of the obtained particles. Moreover, this analysis can measure the size of the nanoparticles in liquid phase, it is possible that nanoparticles are at hydrated states as compared to dry condition in TEM. This typical result is shown in **Figure 5.31**, ZnS nanoparticles synthesized in microemulsion with n-hexanol and  $\text{Cl}^-$  at  $w_o=15$ . Comparing with Figure 5.15a, it can reveal that ZnS nanoparticles in this condition have a size similarly to TEM picture.

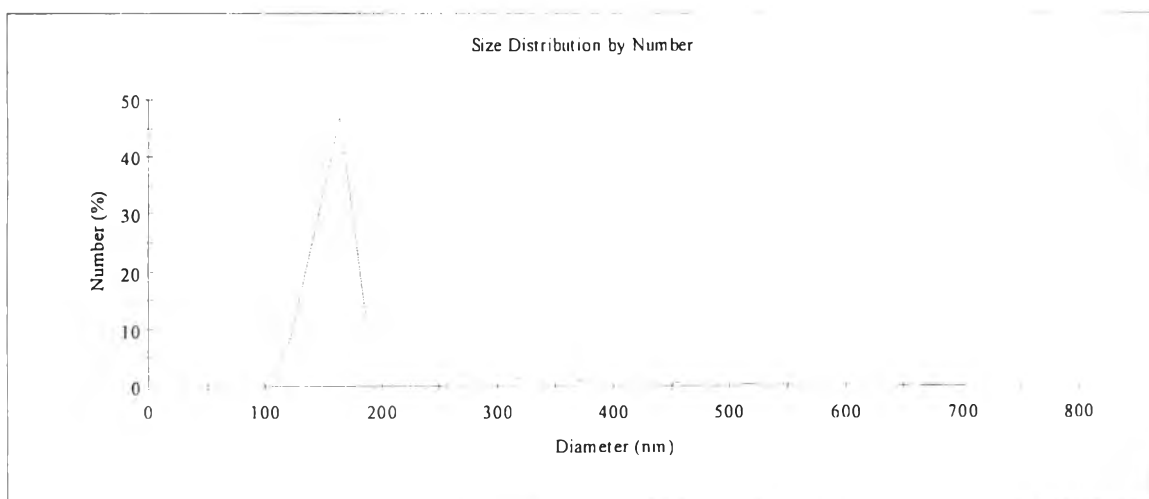


**Figure 5.31** Particle size distribution of ZnS nanoparticles synthesized in microemulsion with n-hexanol as a cosurfactant and  $\text{Cl}^-$  as an anion at  $w_o=15$ .



Some examples of the average size of ZnS nanoparticles that have analogous trend with TEM picture are shown in table 5.1

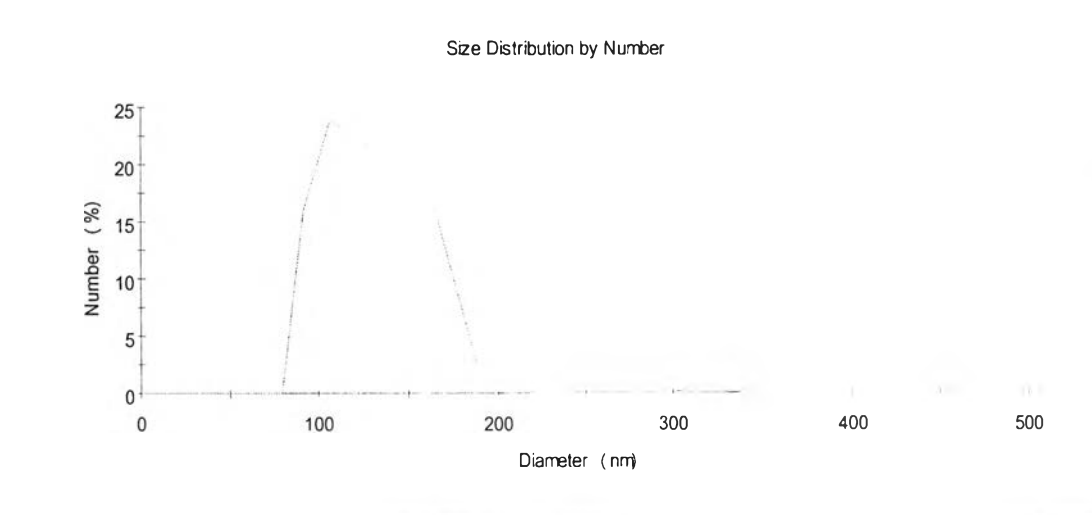


**Figure 5.32** Particle size distribution of ZnS nanoparticles synthesized in microemulsion with n-butanol as a cosurfactant and  $\text{Cl}^-$  as an anion at  $w_0 = 15$ .

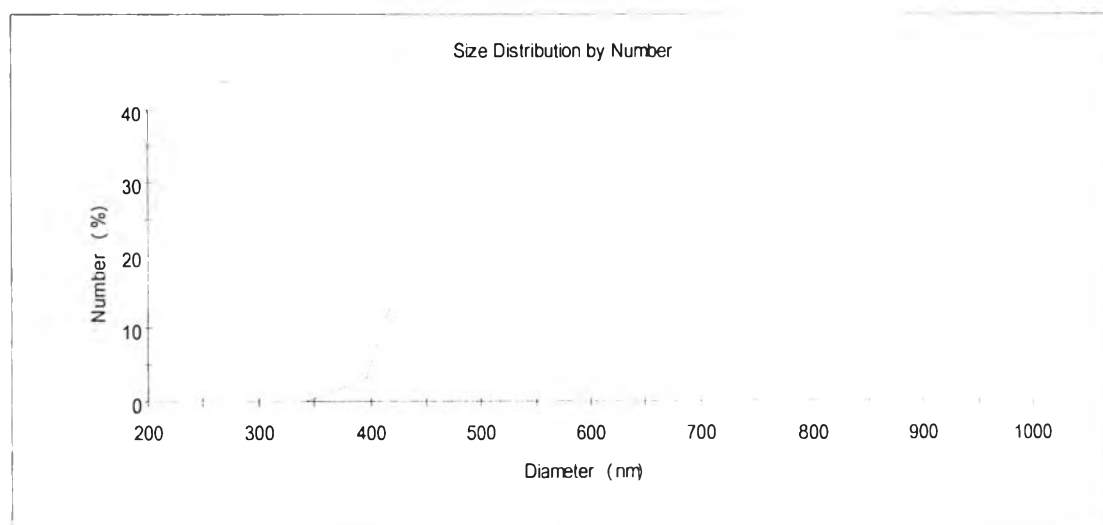


**Figure 5.33** Particle size distribution of ZnS nanoparticles synthesized in microemulsion with n-hexanol as a cosurfactant and  $\text{Br}^-$  as an anion at  $w_0 = 11$ .

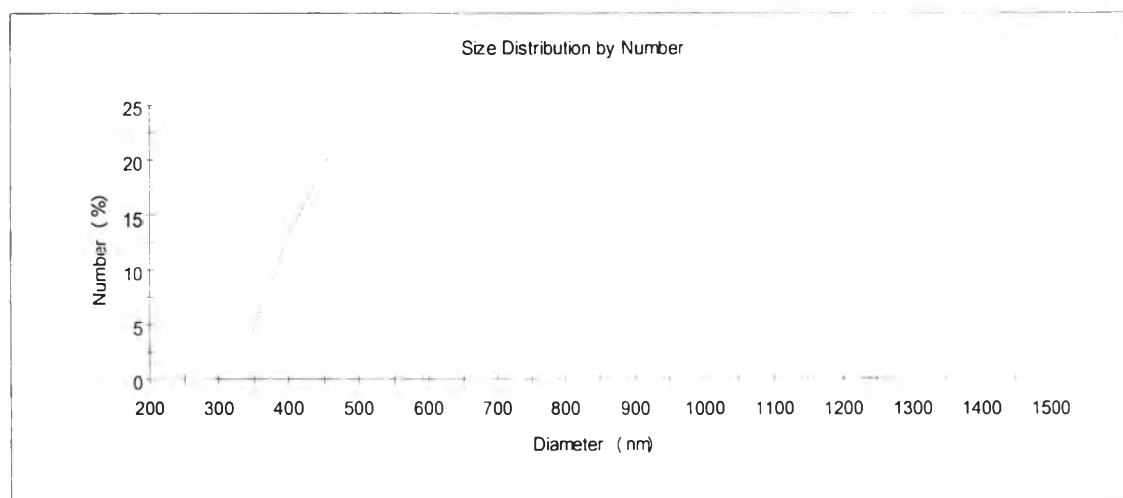


**Figure 5.34** Particle size distribution of ZnS nanoparticles synthesized in microemulsion with n-hexanol as a cosurfactant and  $\text{Br}^-$  as an anion at  $w_0 = 15$ .

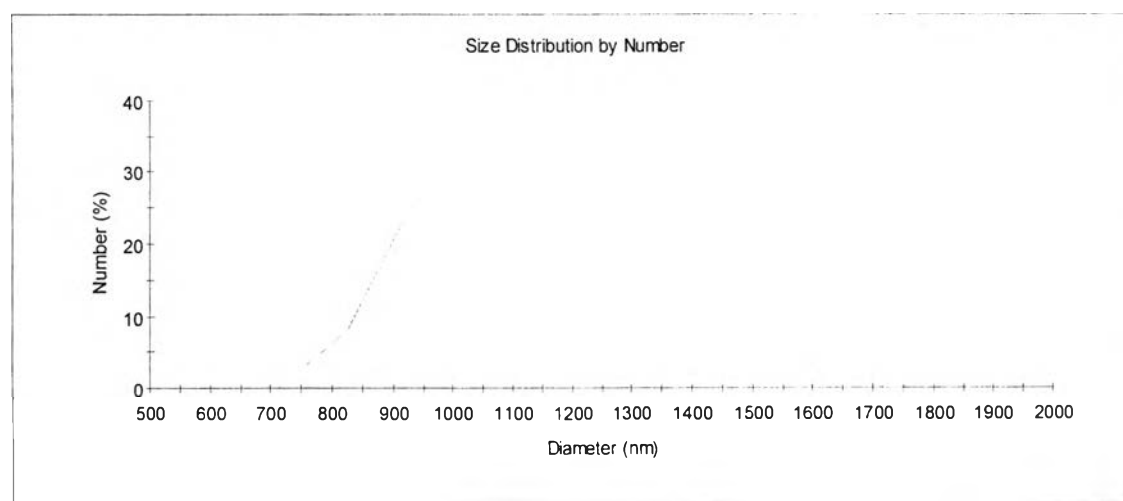


**Figure 5.35** Particle size distribution of ZnS nanoparticles synthesized in microemulsion with n-pentanol as a cosurfactant and  $\text{Br}^-$  as an anion at  $w_0 = 11$ .

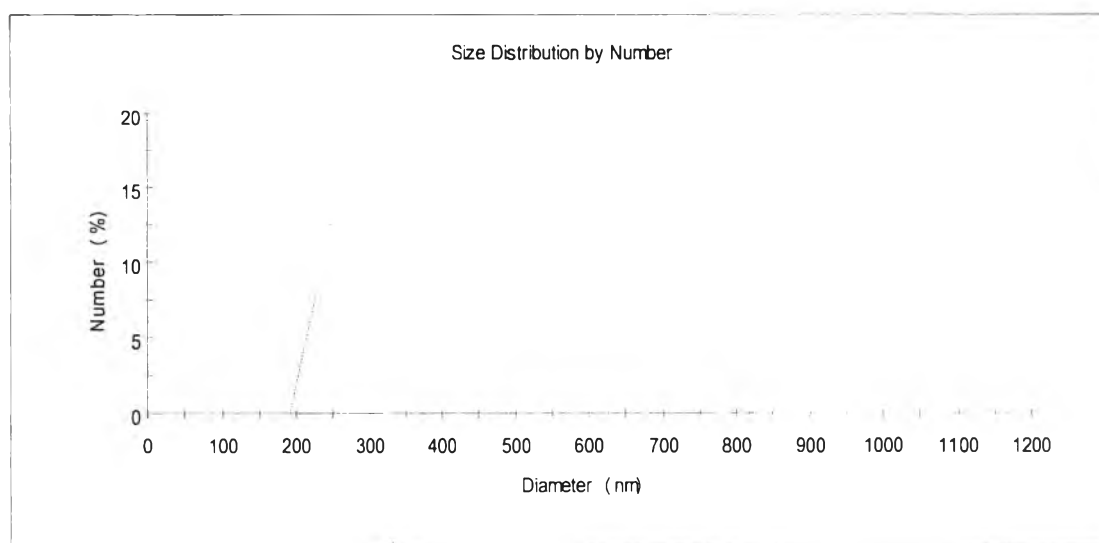


**Figure 5.36** Particle size distribution of ZnS nanoparticles synthesized in microemulsion with n-pentanol as a cosurfactant and  $\text{Br}^-$  as an anion at  $w_0 = 15$ .

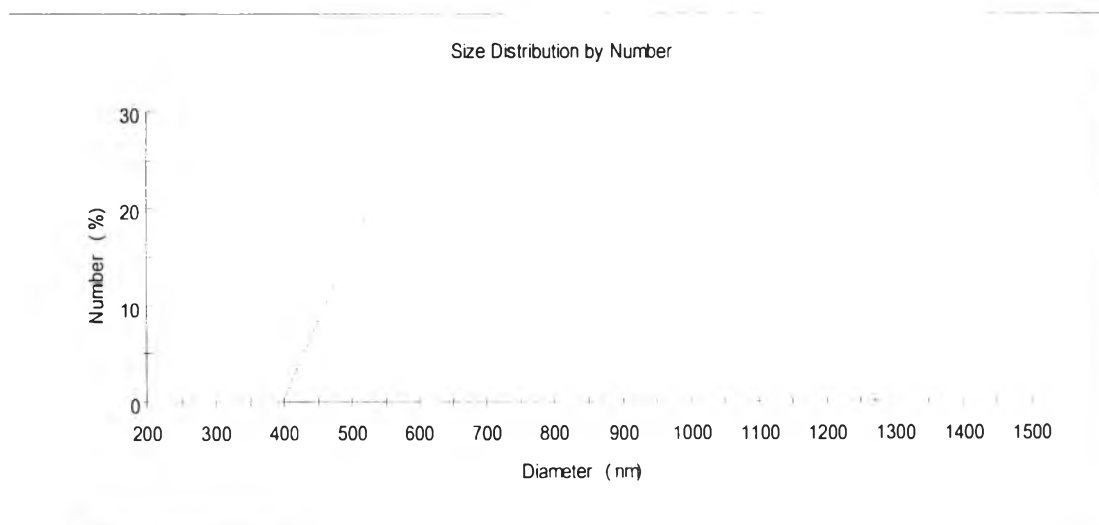


**Figure 5.37** Particle size distribution of ZnS nanoparticles synthesized in microemulsion with n-pentanol as a cosurfactant and  $\text{Br}^-$  as an anion at  $w_0 = 20$ .

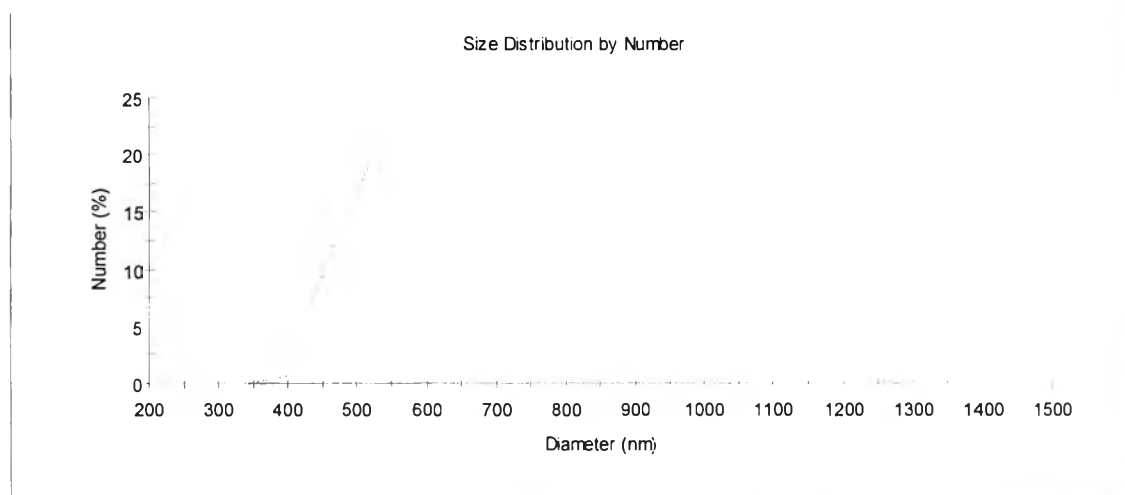


**Figure 5.38** Particle size distribution of ZnS nanoparticles synthesized in microemulsion with n-butanol as a cosurfactant and  $\text{Br}^-$  as an anion at  $w_0 = 11$ .

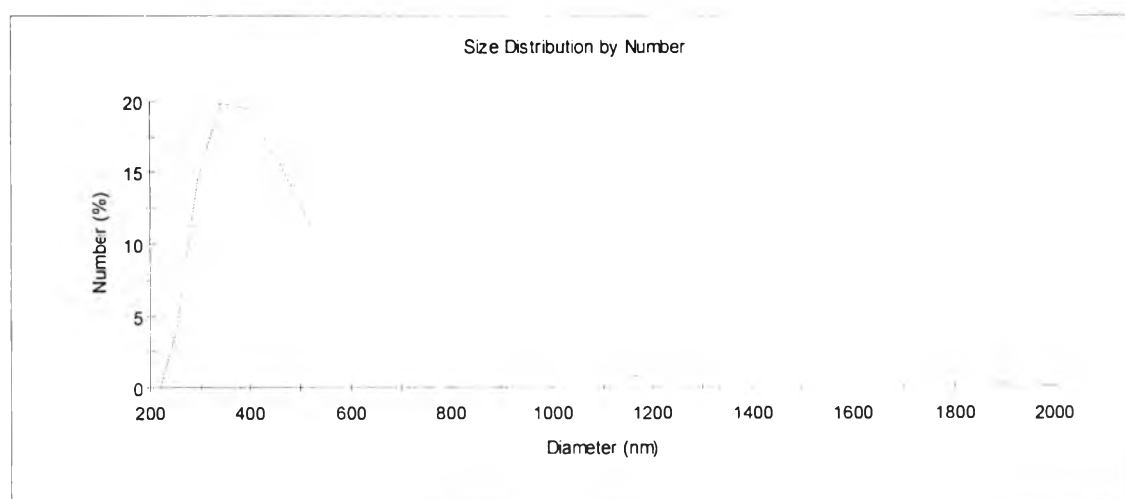


**Figure 5.39** Particle size distribution of ZnS nanoparticles synthesized in microemulsion with n-butanol as a cosurfactant and  $\text{Br}^-$  as an anion at  $w_0 = 15$ .

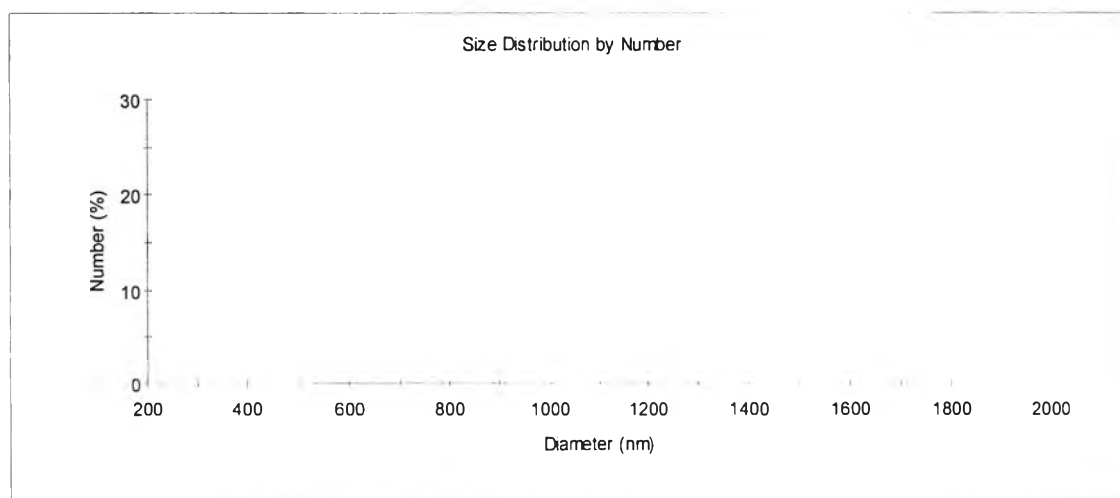


**Figure 5.40** Particle size distribution of ZnS nanoparticles synthesized in microemulsion with n-butanol as a cosurfactant and Br<sup>-</sup> as an anion at  $w_o = 20$ .

**Table 5.1** Typical examples of average size of ZnS nanoparticles obtained from DLS analysis

cosurfactant type	anion type	$w_o$	average size (nm)	Polydispersity index
hexanol	Chloride	7	349.3	0.397
hexanol	Chloride	11	649.4	0.369
hexanol	Chloride	15	314.6	0.207
pentanol	Chloride	11	276.2	0.294
butanol	Chloride	11	243.3	0.421
hexanol	Bromide	11	917.8	0.533
hexanol	Bromide	15	479.5	0.388
pentanol	Bromide	11	783.5	0.363
pentanol	Bromide	15	722.8	0.313
pentanol	Bromide	20	812.2	0.267
butanol	Bromide	11	730.2	0.183
butanol	Bromide	15	641.7	0.412
butanol	Bromide	20	1421	0.529

Table 5.1, demonstrated that the average size of the resulting nanoparticles depends on cosurfactant types,  $w_o$  and anion, For increasing  $w_o$  from 11 to 15, the hydrodynamic diameter of the obtained nanoparticles will slightly decrease. However, further increase  $w_o$  to 20 the average size of nanoparticles will larger than at  $w_o=11$  as shown in Figure 5.38.

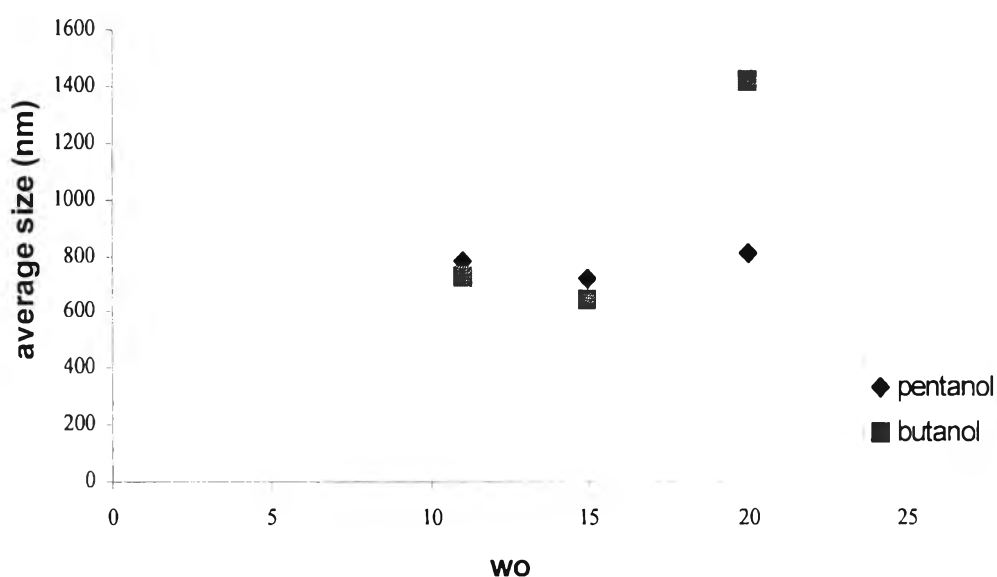


**Figure 5.41** Effect of  $w_o$  on the average size of resulting nanoparticles synthesized in microemulsion with  $\text{Br}^-$  as an anion.

With comparison of the average size of the particles obtained from usage of different cosurfactant types, the nanoparticles synthesized in microemulsion with n-hexanol as a cosurfactant have a size larger than other products synthesized with other cosurfactants at lower  $w_o$  (at 11). This can be explained by a stability of micelle in microemulsion. The larger molecules of cosurfactant posses, the more stability and flexibiliy micelles could exhibit. The nanoparticles can grow larger in these micelles due to their flexibility.

However, according to TEM picture, the average size of nanoparticles from DLS was much larger. This may be due to the agglomeration of ZnS nanoparticles in this mixture, or the sample had some other morphologies of the nanoparticles which could not be investigated by TEM analysis.

However, the size of these nanoparticles depends on their shape at higher  $w_0$ . Also from TEM images, it is demonstrated that ZnS nanoparticles with high aspect ratio can be formed when n-butanol was employed as a cosurfactant. The average size of these nanoparticles in this condition will be larger than others.

For the effect of  $\text{Cl}^-$  and  $\text{Br}^-$ , it is clearly seen that the nanoparticles obtained when  $\text{Cl}^-$  was employed as an anion are smaller than those when using  $\text{Br}^-$ . This may be considered by the agglomeration of these nanoparticles. From the mechanism of agglomerations (Figure 5.11), It is possible that the nanoparticles are harder to agglomerate because there are more impulsion between these micelles when have  $\text{Cl}^-$  in them.